Lipid binding attenuates channel closure of the outer membrane protein OmpF

Idlir Liko[a,b], Matteo T. Degiacomi[a,1,2], Sejeong Lee[a,1], Thomas D. Newport[c], Joseph Gault[a], Eamonn Reading[a,3], Jonathan T. S. Hopper[a,b], Nicholas G. Housden[c], Paul White[c], Matthew Colledge[d], Altin Sula[d], B. A. Wallace[d], Colin Kleanthous[c], Phillip J. Stansfeld[c], Hagan Bayley[a], Justin L. P. Benesch[a], Timothy M. Allison[a,4,5], and Carol V. Robinson[a,b,5]

[a]Department of Chemistry, University of Oxford, Oxford OX1 5QY, United Kingdom; [b]OMass Technologies, Begbroke Science Park, Kidlington OX5 1PF, United Kingdom; [c]Department of Biochemistry, University of Oxford, Oxford OX1 3QU, United Kingdom; and [d]Institute of Structural and Molecular Biology, Birkbeck College, University of London, London WC1E 7HX, United Kingdom

Edited by Michael L. Klein, Temple University, Philadelphia, PA, and approved April 30, 2018 (received for review December 7, 2017)

Strong interactions between lipids and proteins occur primarily through association of charged headgroups and amino acid side chains, rendering the protonation status of both partners important. Here we use native mass spectrometry to explore lipid binding as a function of charge of the outer membrane porin F (OmpF). We find that binding of anionic phosphatidylglycerol (POPG) or zwitterionic phosphatidylcholine (POPC) to OmpF is sensitive to electrospray polarity while the effects of charge are less pronounced for other proteins in outer or mitochondrial membranes: the ferripyoverdine receptor (FpvA) or the voltage-dependent anion channel (VDAC). Only marginal charge-induced differences were observed for inner membrane proteins: the ammonia channel (AmtB) or the mechanosensitive channel. To understand these different sensitivities, we performed an extensive bioinformatics analysis of membrane protein structures and found that OmpF, and to a lesser extent FpvA and VDAC, have atypically high local densities of basic and acidic residues in their lipid headgroup-binding regions. Coarse-grained molecular dynamics simulations, in mixed lipid bilayers, further implicate changes in charge by demonstrating preferential binding of anionic POPG over zwitterionic POPC to protonated OmpF, an effect not observed to the same extent for AmtB. Moreover, electrophysiology and mass-spectrometry–based ligand-binding experiments, at low pH, show that POPG can maintain OmpF channels in open conformations for extended time periods. Since the outer membrane is composed almost entirely of anionic lipopolysaccharide, with similar headgroup properties to POPG, such anionic lipid binding could prevent closure of OmpF channels, thereby increasing access of antibiotics that use porin-mediated pathways.

mass spectrometry | lipids | OmpF

The outer membrane porin F (OmpF) supports passive diffusion of small molecules through the outer membrane. Historically, this trimeric protein was considered to exist only in an open form. As a consequence, permeation through outer membranes was thought to be regulated by modulating the cellular expression level of OmpF or the concentration of charged molecules. Despite OmpF's outer membrane location, surprisingly little or no information is available on its interactions with lipids. Given that previous studies have implicated specific lipids in protein function (1–6), we were curious to know if such lipid-binding sites exist on OmpF, and if so, where they are located and how they might change as a function of pH.

Studies of the distribution of lipid-binding sites in membrane proteins have shown that the interactions of lipid headgroups with a protein are important determinants for lipid binding (6–9). Accordingly, charged amino acids are more likely to be positioned in areas of the protein surface that could interact with lipid headgroups, rather than in hydrophobic transmembrane regions (10, 11). It has also been suggested that, along with physical bilayer properties, charges at protein–lipid interfaces, and the specific locations of amino acids, play important roles in the interactions of membrane proteins with lipids (12). Consistent with this, most X-ray crystal structures of membrane proteins in which lipids have been resolved and modeled show that the lipid–protein interactions are stabilized by polar interactions between lipid headgroups and amino acids on the proteins (12–15). Annular lipid binding may also occur through charge-based interactions between the protein and the lipid headgroup, but in general this type of interaction is more difficult to define given the diffusive nature of the lipid environment.

Native mass spectrometry (MS) has proven useful for studying both specific membrane protein–lipid interactions (16–20) and the annular belts that surround membrane proteins (21). Although the precise mechanistic details of the electrospray process are still

Significance

Outer-membrane porins are often considered as passive conduits of small molecules across lipid bilayers. Using native mass spectrometry experiments we identify a pH-sensitive lipid-binding mechanism of outer membrane porin F, which enables increased threading of a colicin-derived peptide through open channels. Supported by molecular dynamics simulations and channel recording experiments, we posit that this mechanism attenuates channel opening in response to changes in environmental conditions, specifically pH. These findings have important consequences for mass spectrometry experiments, wherein the role of charge is often overlooked, and they also could help provide understanding of antibiotics that gain access to Gram-negative bacteria through porin-mediated pathways.

Author contributions: I.L., M.T.D., P.J.S., H.B., J.L.P.B., T.M.A., and C.V.R. designed research; I.L., M.T.D., S.L., T.D.N., and T.M.A. performed research; J.G., E.R., J.T.S.H., N.G.H., P.W., M.C., A.S., and B.A.W. contributed new reagents/analytic tools; I.L., M.T.D., S.L.,T.D.N., and T.M.A. analyzed data; and I.L., T.M.A., and C.V.R. wrote the paper with contribution from all other authors.

Conflict of interest statement: I.L. and J.T.S.H. are employees of OMass Technologies. Carol Robinson is a cofounder and member of the board of directors of OMass Technologies.

This article is a PNAS Direct Submission.

[1]M.T.D. and S.L. contributed equally to this work.

[2]Present address: Chemistry Department, Durham University, DH1 3LE Durham, United Kingdom.

[3]Present address: Department of Chemistry, Kings College London, WC2R 2LS London, United Kingdom.

[4]Present address: Biomolecular Interaction Centre and School of Physical and Chemical Sciences, University of Canterbury, 8140 Christchurch, New Zealand.

[5]To whom correspondence may be addressed. Email: timothy.allison@canterbury.ac.nz or carol.robinson@chem.ox.ac.uk.

This article contains supporting information online at www.pnas.org/lookup/suppl/doi:10.1073/pnas.1721152115/-/DCSupplemental.

Published online June 11, 2018.

under investigation, the general consensus that emerges is that protein–lipid complexes acquire charge that is proportional to their solvent-accessible surface area (22, 23). During ionization and collisional activation, lipids that could carry a charge in a given polarity (e.g., phosphatidylcholine in positive electrospray polarity) may serve as a charge carrier (24). Effectively, this means that, during the ion generation process, if the protein has sufficient charge, it will relieve Coulombic repulsion through expulsion of charged carriers. This, we postulate, is observed as the reduction in lipid binding in certain combinations of protein, lipid, and electrospray polarity. Since charge underlies the electrospray process, MS is particularly suited to investigating charge-mediated interactions, such as those between the lipid headgroup and the corresponding region of the protein, electrostatic interactions being strengthened in the gas phase (25, 26). Charge-based interactions can be probed by MS through changes in the electrospray polarity under which ions are generated, analogous to changes in pH experienced in solution or in vivo. For example, OmpF, along with other outer membrane proteins, can tolerate pH changes in the range of pH 2–7 (27).

To validate and compare protein lipid-binding properties of OmpF at different pHs, we included additional proteins with different structural features and membrane locations: the ferripyoverdine receptor (FpvA) from *Pseudomonas aeruginosa*, also an outer membrane protein, and the voltage-dependent anion channel (VDAC) from *Homo sapiens* located in the mitochondrial membrane. Three inner membrane proteins were selected: the *Escherichia coli* ammonia channel (AmtB) and the *Mycobacterium tuberculosis* mechanosensitive channel of large conductance (MscL) and the *Magnetococcus* sp. (strain MC-1) voltage-gated sodium channel (NavMS).

We compared the lipid-binding properties of all six membrane proteins under different conditions and developed a computational algorithm to define the lipid-binding headgroup regions of all membrane proteins in the Protein Data Bank. We then correlated changes in lipid-binding properties with different charged residue distributions in the critical regions identified. We validated our findings with coarse-grained molecular dynamics simulations and single-channel recording experiments. Together, this integrative approach has allowed us to define a role for specific lipid binding to OmpF at low pH: maintaining open states of an outer membrane porin for increased passage of small molecules including antibiotics.

Results

Lipid Binding to OmpF Is Sensitive to Changes in the Electrospray Polarity. To investigate the sensitivity of lipid binding to OmpF to charge, we first purified the protein to remove remaining endogenous lipids. OmpF was then incubated with the anionic lipid phosphatidylglycerol (POPG) (10-fold excess over protein). Mass spectra in octyl glucoside were recorded in both positive and negative electrospray polarities (Fig. 1 *A* and *B*). Additional adduct peaks on the charge state series for the OmpF trimer were assigned to binding of POPG. Surprisingly, when the electrospray polarity was switched to the negative-ion mode, using the same protein–lipid solution and nano-electrospray tip, no POPG binding was observed. Selecting next the neutral zwitterionic lipid phosphatidylcholine (POPC), we found that, for negatively charged OmpF, multiple POPC lipids (fewer than four) could be observed bound to OmpF, while no binding was observed when the electrospray polarity was switched back to positive.

To examine if this dramatic sensitivity to charge was a general phenomenon or specific to OmpF, we selected AmtB, incubating it with POPC or POPG. In this case, lipids could be observed bound both to positively or negatively charged protein with approximately equal intensity (Fig. 1 *C* and *D*). Extending our investigations to MscL, a protein known to sense and respond to membrane tension (28), we found only a moderate difference in the extent of lipid binding in the spectra recorded under the two different polarities (*SI Appendix*, Fig. S1). Three more membrane proteins were investigated: NavMS, FpvA, and VDAC. For NavMS, a low level of POPG was detected binding to negatively charged protein, while POPC was observed bound only to negatively charged NavMS (*SI Appendix*, Fig. S1). Intriguingly,

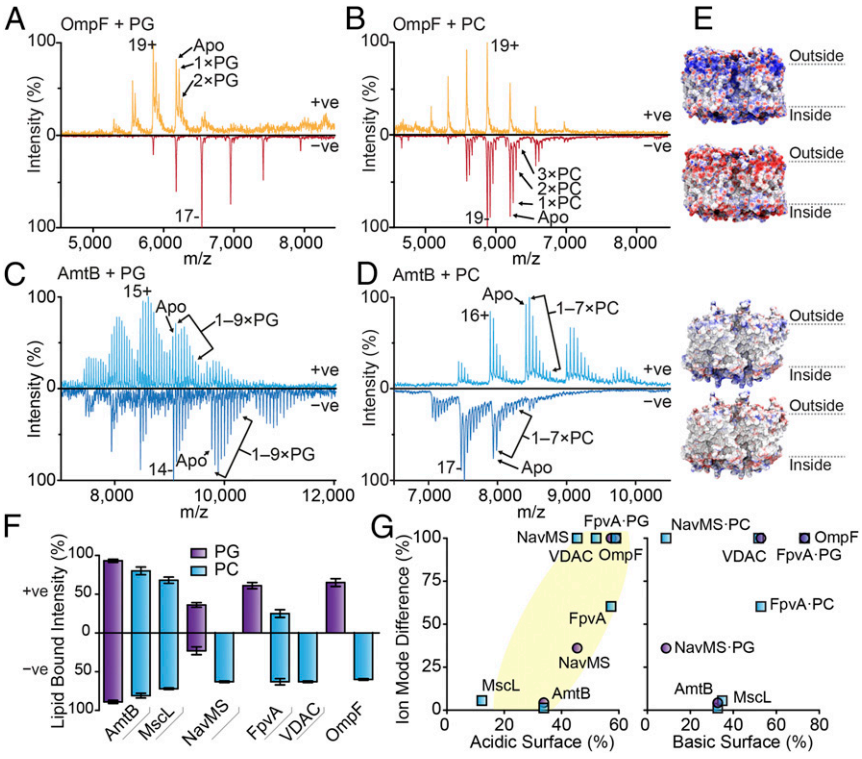

Fig. 1. Native mass spectra of lipid binding to positively and negatively charged membrane proteins. (*A–D*) For each protein, spectra were recorded from the same electrospray needle under similar instrument activation conditions. The *Top* spectrum in each panel was recorded with positive electrospray polarity while the *Bottom* spectrum was recorded with negative electrospray polarity. Discrete peaks are labeled, although in some cases more lipid binding is visible. (*E*) The corresponding protein surfaces are colored according to electrostatic charges at low and high pH for positive and negative ion modes, respectively. The color ranges were set from −20 (red) to 20 (blue). (*F*) Lipid binding as a percentage of the total intensity in positive (*Top*) and negative (*Bottom*) ion modes. Magnitude is dependent upon experimental conditions. (*G*) Relative difference in ion mode lipid-binding percentage as a function of acidic (*Left*) or basic (*Right*) surface area. A positive correlation between acidic or basic residues and difference in lipid binding as a function of charge is observed for acidic residues (highlighted yellow).

FpvA showed low levels of POPG binding, but high levels of binding to POPC (>3 lipid molecules) when negatively charged (*SI Appendix*, Fig. S1). MscL, on the other hand, could be seen bound to POPC in both polarities, while VDAC was observed bound only to POPC when negatively charged. Given that the same lipids were used in all experiments, and therefore subject to the same charging conditions, survival of the differing interactions must arise from the distribution of chargeable residues in the various proteins.

Plotting the extent of lipid binding as a function of the different electrospray polarities under which the six membrane proteins were investigated reveals three distinct categories (Fig. 1*F*): (*i*) a category in which lipids were observed bound to an approximately equal extent when positively or negatively charged (e.g., AmtB); (*ii*) a category in which lipids were observed bound in one electrospray polarity and noticeably less in the other (e.g., NavMS); and (*iii*) a category in which lipid binding was observed in one electrospray polarity but undetected in the other (e.g., OmpF).

In summary, AmtB is an example of a protein that showed little change in lipid binding as a function of electrospray polarity whereas OmpF showed the greatest sensitivity. Comparing the electrostatic surfaces of the two proteins, generated at artificially low and high pH to mimic the positive and negative ion electrospray polarities of the mass spectrometer, a large shift in the charge carriers from acidic to basic residues was observed for OmpF whereas only a modest shift was observed for AmtB. We conclude that the dramatic changes in lipid binding arise as a function of the differing degrees of change and distribution of charges induced by protonation or deprotonation events (Fig. 1*G*).

Locating Chargeable Residues Positioned for Lipid Binding. To see how charge density in the lipid headgroup-binding region varied across a wide range of membrane proteins, we exploited a database that predicts the alignment of all of the transmembrane proteins currently available in the Protein Data Bank of Transmembrane Proteins (PDBTM) with a synthetic lipid bilayer (29). We aligned 2,063 structures according to PDBTM and subsequently studied their surface in regions expected to interact with lipid headgroups. We first simulated the predicted lipid headgroup regions of the membrane as two layers of mesh points. Any mesh point clashing with a protein atom or located in a protein internal cavity (e.g., a channel) was removed (Fig. 2*A*). We then calculated the solvent-accessible surface area of all protein atoms within 4 Å from each mesh. The percentage of this surface featuring amino acids capable of picking up a positive charge (defined as "basic") or releasing one ("acidic") was then calculated.

We first determined the total surface percentage composed of basic or acidic residues for each protein using the two surface regions corresponding to the inside and outside of the protein (Fig. 2*B*). We found an average total for acidic residues of 27 ± 15% and for basic residues of 39 ± 17%. This wide range of values for both residue types suggests that there is a slight preference for basic residues. Next we determined whether a different secondary structure leads to the presentation of specific lipid-interacting headgroups. We therefore extracted from our dataset subsets of α-helical (1,769 entries) and β-sheet (294) proteins. Interestingly, outer membrane proteins (which comprise almost exclusively the set of β-sheet proteins) typically have more acidic and basic residues than their inner membrane counterparts, which are typically α-helical (Fig. 2*B*).

We then considered differences in residue composition on either side of the membrane, that is, whether a high relative surface area of either acidic or basic residues on one side of the protein was correlated with a large difference on the opposing side. Within the dataset we found proteins where the distribution of chargeable residues was symmetric and others where it was highly asymmetric (*SI Appendix*, Figs. S2 and S3). This suggests that the residues interacting with the lipid headgroups are not generally paired with potential bilayer asymmetries or affected by protein topology. Interestingly, some proteins (OmpF, VDAC, and FpvA studied here) have a high contribution of chargeable residues in these surface areas. We hypothesize that these dense regions of highly charged residues lead to the observed lipid-binding sensitivity associated with changes in protonation.

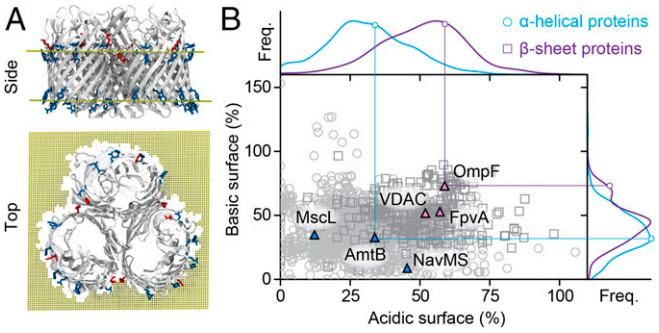

Fig. 2. Analysis of structures in the PDBTM to determine the surface area contribution of acidic and basic residues to the lipid headgroup-binding region. (*A*) The analysis process first aligned each membrane protein structure to determine the region of the protein proximal to the lipid headgroups in a lipid bilayer. The proportion of the surface area of this region contributed by either acidic or basic residues was calculated. (*B*) All membrane protein structures analyzed (n = 2,064) for acidic and basic residue contribution. The β-sheet/outer membrane proteins (gray squares) have more acidic or basic residues in the lipid headgroup-binding region than α-helical membrane proteins (gray circles). The surface area contribution was calculated for both the inside and the outside lipid headgroup-binding regions, and these two values were summed for each protein. The set of annotated outer membrane proteins is identical to those classified as β-sheet, with the exception of the addition of structures of hemolysin. Membrane proteins analyzed by native MS to investigate lipid binding are independently plotted (triangles) and colored according to the protein type (α-helical, blue; β-sheet, pink). The locations of AmtB and OmpF are denoted. Axes are decorated with histograms (bin size of 2) of distribution of proteins with different surface-area contributions, smoothed by applying a kernel-density estimate using Gaussian kernels.

pH Sensitivity to Lipid-Binding Preferences. Working on the hypothesis that a high local density of acidic residues in OmpF will lose negative charge to become neutral and thereby exhibit pH-sensitive lipid binding, we compared OmpF with AmtB in silico mimicking these low-pH conditions. We set up a series of coarse-grained molecular dynamics (MD) simulations of both proteins in mixed bilayers composed of equal quantities of POPC and POPG and mimicked both deprotonated and protonated states. To approximate protonation, negatively charged side-chain beads of aspartic and glutamic acid residues and negatively charged lipid phosphate groups were neutralized, and a positive charge was applied to a side-chain bead of each histidine.

Five separate 1-μs simulations were performed for both proteins in both states, and occupancy of POPG molecules as a fraction of total lipid occupancy (POPG and POPC) within 6 Å of the protein (corresponding to the first annular shell, *SI Appendix*, Fig. S4) was measured for each acidic residue. Both AmtB and OmpF show an increase in POPG fraction in the protonated state; however, POPG binding is substantially more pronounced in the case of OmpF (Fig. 3 and *SI Appendix*, Fig. S5). To examine more localized changes in patterns of binding, we examined changes in the lipid-binding preferences on a 2D grid over the upper and lower leaflets of each protein. In both cases, the net shift in lipid-binding preferences comprises both local increases and decreases in POPG fraction, as would be

expected (Fig. 3). In the case of OmpF, shifts occurring upon protonation differ greatly between leaflets, with OmpF in the upper leaflet attracting POPG and the lower leaflet shifting more toward POPC. However, for the latter, apparent changes in bulk lipid regions are less relevant, and there remains a change in POPG in proximity to the acidic residues.

In summary, the simulations suggest that the positioning of acidic residues in the lipid headgroup-binding region of OmpF, particularly the upper leaflet, affect its lipid-binding preference depending on protonation conditions. These MD results corroborate the effects of acidic residues on lipid binding observed in our native MS experiments, suggesting that the high density of chargeable residues in OmpF affect lipid-binding preferences in the context of a membrane bilayer.

POPG Stabilizes OmpF in an Open Conformation. Given the results from native MS and MD simulations that suggest that POPG–OmpF interactions persist at low pH, we examined the effect of POPG on the conductance and gating of OmpF. We reconstituted OmpF trimer in a planar lipid bilayer membrane in which each monomer can be observed and lipid composition can be modulated (30, 31). We first used symmetric bilayers of DPhPC, a lipid commonly used in planar lipid bilayer measurements with the same overall neutral, zwitterionic headgroup as POPC, compared with the net negative charge of POPG. The mean unitary conductance of OmpF in a pure DPhPC bilayer was 1.3 ± 0.2 nS (n = 19) per monomer (Fig. 4*A*), identical to the known value (32). In the presence of 25% POPG at pH 4, the unitary conductance value increased slightly by 7% to 1.4 ± 0.1 nS (n = 15) (Fig. 4*A*); meanwhile, at pH 8 the conductance value of OmpF remained unchanged in the presence of POPG (*SI Appendix*, Fig. S6). This provided an initial suggestion that the presence of POPG in DPhPC bilayers may increase ion flow through OmpF in acidic conditions.

To investigate the pore dynamics in more detail, channel gating was examined under the action of an applied potential at 100 mV. Due to the acidic conditions at pH 4, a voltage was applied that was lower than the critical voltage for closure (~ ±130 mV) (33). The characteristic three-step opening and closing of OmpF was monitored until all three subunits had closed—as indicated by a decrease in the current to almost zero (Fig. 4 *B* and *D*). In DPhPC bilayers, the mean closure time for OmpF from the fully open state (O3) to the fully closed state (C) was measured as 54.3 s (n = 11) by fitting to an exponential distribution. In the presence of POPG (25%), the mean closure time increased to 175.8 s (n = 10). This threefold increase (P value of 0.023) suggests that POPG helps to stabilize OmpF in an open state (Fig. 4*C*).

By examining the closure steps in more detail, the presence of POPG was specifically found to influence two closing steps (O2 → O1 and O1 → C) (*SI Appendix*, Fig. S7 and Table S2). The mean closing time for these two steps also increased to be threefold larger in the presence of POPG from 4.9 to 13.1 s and from 17.9 to 48 s, respectively (P values 0.015 and 0.044, respectively), and a higher probability of reopening (O2 → O3 and O1 → O2) was also observed (*SI Appendix*, Fig. S8). In the presence of POPG, the reopening of the single-subunit closed state of OmpF (O2 → O3) occurred for 70% of the pores analyzed (7/10), compared with only 10% (1/11 pores analyzed) in the absence of POPG. Taken together, this indicates that the presence of POPG lipid in the membrane not only helps maintain an open pore conformation but also promotes the reopening of closed pores. These quantitative analyses reveal that POPG influences the voltage-induced gating of OmpF at low pH and promotes a threefold change in the delay of closing.

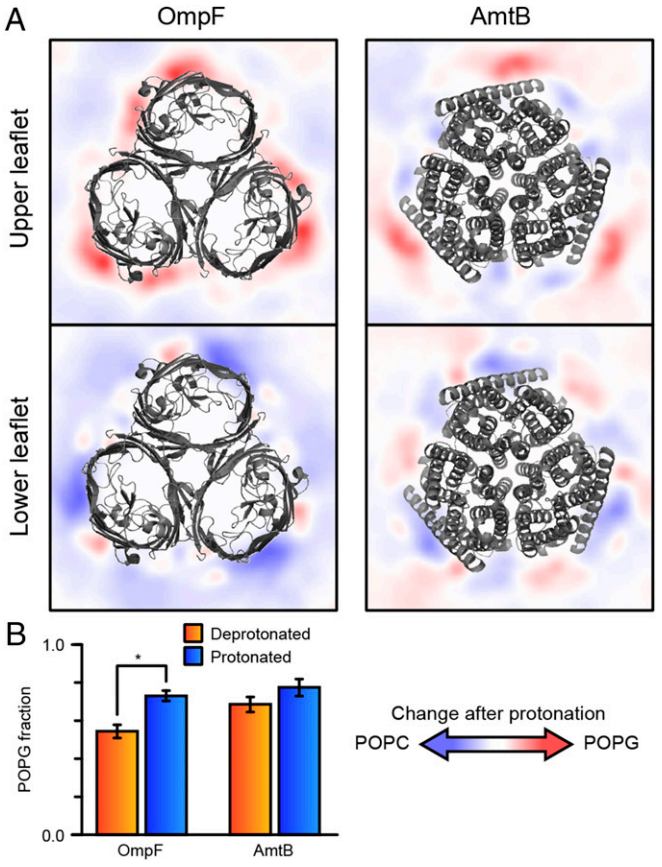

Fig. 3. Coarse-grained molecular dynamics simulations of AmtB and OmpF in mixed bilayers of POPC and POPG. (*A*) Changes in lipid-binding preferences after protonation. The membrane proteins are in a cartoon representation colored gray. (*B*) The relative binding preferences for POPG (over POPC) calculated as the fraction of total lipid occupancy for OmpF and AmtB toward acidic residues in different protonation conditions. Error bars represent SD from five simulations. The change in POPG fraction for OmpF is significantly different (P value < 0.0001) as indicated by a single asterisk, whereas in the case of AmtB the change in POPG fraction prior and after protonation was not statistically different (P value < 0.74).

Probing the Open Pores. Aside from its role in the passive diffusion of small molecules through the outer membrane, OmpF also forms part of a cytotoxic translocon complex, through which the nuclease colicin ColE9 threads to initiate cell entry and ultimately death (34). The intrinsically unstructured translocation domain of ColE9 has two OmpF-binding sites in its sequence (OBS1 and OBS2), and these sequences as peptides can be observed to bind to OmpF inside the pores within the trimer. Access to the peptide-binding sites inside the pores may be affected by the extracellular loops, and since the electrophysiology experiments clearly demonstrate a change in gating behavior in the presence of POPG, we hypothesized that the OmpF–OBS1 interaction may also be influenced by POPG binding. Using high-resolution native MS (35), we analyzed the relative binding of the OBS1 peptide to different lipid-bound forms of OmpF. Notably, we observed that POPG-bound OmpF binds OBS1 more than POPG-free OmpF (Fig. 4*E* and *SI Appendix*, Fig. S9), suggesting that POPG increases the apparent affinity of the protein for the peptide. This direct evidence supports a scenario where interactions between OmpF and POPG stabilize the open conformation of the pore. This suggests that in vivo OmpF function can be fine-tuned by lipid interactions.

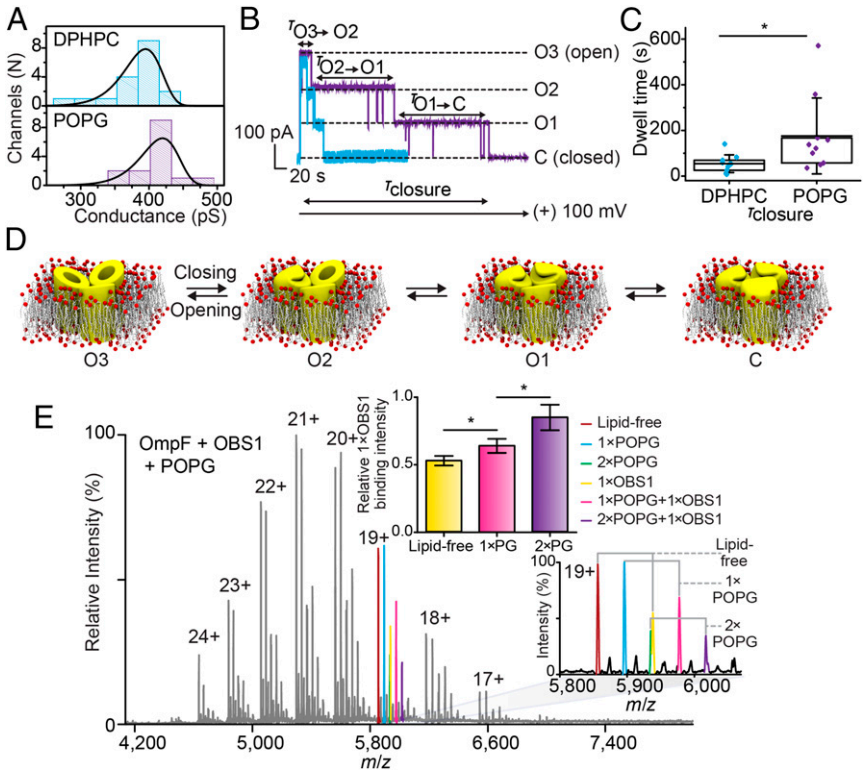

Fig. 4. The influence of the negatively charged lipid, POPG, on OmpF porin gating at low pH. (*A*) OmpF channel conductance values (all three pores open) in 1 M KCl at pH 4.0 at +100 mV were obtained in DPhPC planar bilayers (blue) and in DPhPC/POPG (3:1 ratio) bilayers (purple) with 19 and 15 independent OmpF porins, respectively. The mean conductance value of the fully open OmpF channel was 1.3 ± 0.2 nS (n = 19) per monomer in a DPhPC bilayer and 1.4 ± 0.1 nS (n = 15) in a DPhPC/POPG bilayer. (*B*) Representative current versus time traces for a single OmpF porin in a DPhPC bilayer (purple) and in a DPhPC/POPG (3:1) bilayer (blue). A trans potential of +100 mV was applied until all of the pores had closed. (*C*) Box and whisker plot of closure times. The top and bottom lines of a box enclose values in the range encompassing 25–75% of the values. The mean closure times are shown as black lines within the boxes and are significantly different as determined by Mann–Whitney U test (P value < 0.021). (*D*) Schematic showing stepwise OmpF gating. The resulting states of OmpF are O3 (three pores open), O2 (two pores open), O1 (one pore open), and C (all closed). (*E*) High-resolution native MS of OmpF in the presence of OBS1 (10 μM) and POPG (100 μM) (*Left*). A range of bound forms are observed in the spectrum of single- and double-peptide and lipid-binding combinations. (*Inset*) Expansion of charge state 19+. Bar chart of relative peak intensities indicates that a peptide cobound with POPG is observed to a greater extent than bound alone. The mean relative binding intensities are significantly different in the different lipid-bound forms (P values of 0.0008 and 0.027).

Discussion

Building upon previous investigations (6, 7), we have shown that the headgroup interactions of lipids can play a role in the direct interaction of lipids with membrane proteins. As a corollary, the membrane protein surfaces that interact with lipid headgroups can regulate the selectivity of lipid binding. Interestingly, we found that different classes of membrane proteins have different distributions of acidic and basic residues in these binding areas. Outer membrane proteins tend to possess lipid headgroup-binding surfaces composed of a higher concentration of both acidic and basic residues, suggesting that there may be more pronounced differences in lipid-binding behavior. In line with this, we found that membrane proteins with representatively high concentrations of acidic residues in these regions showed lipid binding by native MS that was dependent on the combination of lipid and electrospray polarity. Therefore, to probe membrane protein–lipid interactions by native MS, and to examine a full range of lipid-binding interactions, an appropriate choice of electrospray polarity is necessary and will be particularly important for proteins with high percentages of chargeable residues in the headgroup-binding regions.

We probed how lipid-binding preferences may differ in response to changing pH by performing MD simulations and electrophysiology experiments. OmpF has the greatest surface area of chargeable residues and showed the most differences in lipid binding as assessed by native MS, as well as enhanced POPG binding in molecular dynamics simulations. POPG binding to OmpF at the single-channel level showed enhanced ion transport activity as indicated by the increase in conductance and the prolonged open state under applied potentials. This could result from the electrostatic interactions between the net negative charge of the lipid headgroup and the chargeable residues at the surface of OmpF (36–38). pH changes and mutations of charged residues in extracellular loops have been shown to affect the voltage-induced gating (32, 39–44). This supports the idea that the stabilized OmpF open state, in POPG-containing bilayers, is induced by electrostatic interactions, leading to a conformational change of the extracellular surface of OmpF.

We observed that under low-pH conditions, OmpF, which has a large proportion of acidic residues in its lipid headgroup-binding region, can subtly change lipid-binding preferences. This means that this protein could respond to pH changes by recruiting a different cohort of annular lipids, which in turn could affect their stability or function. Considering the composition of the lipids in the outer leaflet of the outer membrane of *E. coli*, a high proportion of LPS is anticipated, with recent evidence also suggesting the presence of other anionic lipids (45, 46). Given that the headgroup chemistry of LPS is analogous to POPG under neutral, positive, and negative ion modes (*SI Appendix*, Fig. S3), the charge effects of POPG binding are likely to be analogous to those of LPS binding. Using the effects of POPG as a mimetic for LPS, we considered binding at low pH and

further explored the effects of lipid binding on channel closing by binding of the translocon-derived peptide OBS1. Results showed that the extent of peptide threading through the open channels can be affected by the binding of the lipid POPG under low-pH conditions. The stability and interactions of OmpF thus appear to be influenced by lipid binding. Since both POPG and LPS are without formal charge at low pH, we propose that both lipids would enable channels to remain open for extended time periods, enabling increased peptide threading.

Taken together, these MS, computational, and conductivity measurements have therefore uncovered how lipids may regulate OmpF through the ability of the techniques to highlight and explore the allosteric effects of lipid binding. The ability of OmpF closure to be modulated by lipid binding is likely an important feature of outer membrane permeability (47). The finding that lipids can regulate closure of OmpF is important, therefore, since such regulation may well increase penetration of antibiotics using porin-mediated pathways.

Methods

Extended experimental and method details can be found in *SI Appendix*. Membrane protein structures were sourced from the PDBTM and used to calculate the surface area contributions of chargeable residues in the lipid headgroup-binding region. For native MS analysis, membrane proteins were overexpressed in bacterial cell lines, purified, and exchanged to 200 mM ammonium acetate, pH 7.4, supplemented with twice the critical micelle concentration of the detergent of choice in the presence of POPC or POPG lipids. Spectra were recorded in both positive and negative electrospray polarity using Synapt G1 (Waters) and Q Exactive hybrid quadrupole-Orbitrap (ThermoFisher Scientific) mass spectrometers. Current measurements were recorded using a patch clamp amplifier (Axopatch 200B; Axon Instruments) after OmpF was reconstituted in planar bilayers composed of either DPhPC or a mixture of DPhPC and POPG in 20 mM sodium acetate and 1 M KCl at pH 4. Lipid interactions with OmpF and AmtB were simulated using coarse-grained molecular dynamics in membranes composed of POPC and POPG in protonated and deprotonated states with the MemProtMD pipeline.

ACKNOWLEDGMENTS. We thank members of the C.V.R. laboratory for helpful discussions. Research in the C.V.R. laboratory is supported by Wellcome Trust Senior Investigator Award 104633/Z/14/Z and by Biological Science Research Council (BBSRC) Grant BB/L021234/1 (to C.K. and H.B.). This work was also supported, in part, by BBSRC Grants BB/L006790 and BB/L026251 (to B.A.W.). M.C. was supported by a Medical Research Council Collaborative Awards in Science and Engineering studentship. J.G. is a Junior Research Fellow of The Queen's College, Oxford.

1. Heginbotham L, Kolmakova-Partensky L, Miller C (1998) Functional reconstitution of a prokaryotic K+ channel. *J Gen Physiol* 111:741–749.
2. Valiyaveetil FI, Zhou Y, MacKinnon R (2002) Lipids in the structure, folding, and function of the KcsA K+ channel. *Biochemistry* 41:10771–10777.
3. Starling AP, Dalton KA, East JM, Oliver S, Lee AG (1996) Effects of phosphatidylethanolamines on the activity of the Ca(2+)-ATPase of sarcoplasmic reticulum. *Biochem J* 320:309–314.
4. Dalton KA, Pilot JD, Mall S, East JM, Lee AG (1999) Anionic phospholipids decrease the rate of slippage on the Ca(2+)-ATPase of sarcoplasmic reticulum. *Biochem J* 342: 431–438.
5. Pilot JD, East JM, Lee AG (2001) Effects of phospholipid headgroup and phase on the activity of diacylglycerol kinase of Escherichia coli. *Biochemistry* 40:14891–14897.
6. Powl AM, East JM, Lee AG (2008) Importance of direct interactions with lipids for the function of the mechanosensitive channel MscL. *Biochemistry* 47:12175–12184.
7. Hakizimana P, Masureel M, Gbaguidi B, Ruysschaert JM, Govaerts C (2008) Interactions between phosphatidylethanolamine headgroup and LmrP, a multidrug transporter: A conserved mechanism for proton gradient sensing? *J Biol Chem* 283: 9369–9376.
8. Soubias O, Teague WE, Jr, Hines KG, Mitchell DC, Gawrisch K (2010) Contribution of membrane elastic energy to rhodopsin function. *Biophys J* 99:817–824.
9. Vorobyov I, Allen TW (2011) On the role of anionic lipids in charged protein interactions with membranes. *Biochim Biophys Acta* 1808:1673–1683.
10. Ulmschneider MB, Sansom MS (2001) Amino acid distributions in integral membrane protein structures. *Biochim Biophys Acta* 1512:1–14.
11. von Heijne G (2006) Membrane-protein topology. *Nat Rev Mol Cell Biol* 7:909–918.
12. Contreras FX, Ernst AM, Wieland F, Brügger B (2011) Specificity of intramembrane protein-lipid interactions. *Cold Spring Harb Perspect Biol* 3:a004705.
13. Morita M, et al. (2011) Lipid recognition propensities of amino acids in membrane proteins from atomic resolution data. *BMC Biophys* 4:21.
14. Norimatsu Y, Hasegawa K, Shimizu N, Toyoshima C (2017) Protein-phospholipid interplay revealed with crystals of a calcium pump. *Nature* 545:193–198.
15. Palsdottir H, Hunte C (2004) Lipids in membrane protein structures. *Biochim Biophys Acta* 1666:2–18.
16. Laganowsky A, et al. (2014) Membrane proteins bind lipids selectively to modulate their structure and function. *Nature* 510:172–175.
17. Allison TM, et al. (2015) Quantifying the stabilizing effects of protein-ligand interactions in the gas phase. *Nat Commun* 6:8551.
18. Liko I, et al. (2016) Dimer interface of bovine cytochrome c oxidase is influenced by local posttranslational modifications and lipid binding. *Proc Natl Acad Sci USA* 113: 8230–8235.
19. Habeck M, Kapri-Pardes E, Sharon M, Karlish SJ (2017) Specific phospholipid binding to Na,K-ATPase at two distinct sites. *Proc Natl Acad Sci USA* 114:2904–2909.
20. Patrick JW, et al. (2018) Allostery revealed within lipid binding events to membrane proteins. *Proc Natl Acad Sci USA* 115:2976–2981.
21. Bechara C, et al. (2015) A subset of annular lipids is linked to the flippase activity of an ABC transporter. *Nat Chem* 7:255–262.
22. Reading E, et al. (2015) The role of the detergent micelle in preserving the structure of membrane proteins in the gas phase. *Angew Chem Int Ed Engl* 54:4577–4581.
23. Morgner N, Montenegro F, Barrera NP, Robinson CV (2012) Mass spectrometry: From peripheral proteins to membrane motors. *J Mol Biol* 423:1–13.
24. Hogan CJ, Jr, Carroll JA, Rohrs HW, Biswas P, Gross ML (2009) Combined charged residue-field emission model of macromolecular electrospray ionization. *Anal Chem* 81:369–377.
25. Robinson CV, et al. (1996) Probing the nature of noncovalent interactions by mass spectrometry. A study of protein-CoA ligand binding and assembly. *J Am Chem Soc* 118:8646–8653.
26. Yin S, Xie Y, Loo JA (2008) Mass spectrometry of protein-ligand complexes: Enhanced gas-phase stability of ribonuclease-nucleotide complexes. *J Am Soc Mass Spectrom* 19: 1199–1208.
27. Foster JW (2004) Escherichia coli acid resistance: Tales of an amateur acidophile. *Nat Rev Microbiol* 2:898–907.
28. Iscla I, Blount P (2012) Sensing and responding to membrane tension: The bacterial MscL channel as a model system. *Biophys J* 103:169–174.
29. Ikeda M, Arai M, Okuno T, Shimizu T (2003) TMPDB: A database of experimentally-characterized transmembrane topologies. *Nucleic Acids Res* 31:406–409.
30. Bayley H, Cremer PS (2001) Stochastic sensors inspired by biology. *Nature* 413: 226–230.
31. Pliotas C, et al. (2015) The role of lipids in mechanosensation. *Nat Struct Mol Biol* 22: 991–998.
32. Nestorovich EM, Rostovtseva TK, Bezrukov SM (2003) Residue ionization and ion transport through OmpF channels. *Biophys J* 85:3718–3729.
33. Baslé A, Iyer R, Delcour AH (2004) Subconductance states in OmpF gating. *Biochim Biophys Acta* 1664:100–107.
34. Housden NG, et al. (2013) Intrinsically disordered protein threads through the bacterial outer-membrane porin OmpF. *Science* 340:1570–1574.
35. Gault J, et al. (2016) High-resolution mass spectrometry of small molecules bound to membrane proteins. *Nat Methods* 13:333–336.
36. Samartzidou H, Delcour AH (1998) E.coli PhoE porin has an opposite voltage-dependence to the homologous OmpF. *EMBO J* 17:93–100.
37. Conlan S, Zhang Y, Cheley S, Bayley H (2000) Biochemical and biophysical characterization of OmpG: A monomeric porin. *Biochemistry* 39:11845–11854.
38. Pezeshki S, Chimerel C, Bessonov AN, Winterhalter M, Kleinekathöfer U (2009) Understanding ion conductance on a molecular level: An all-atom modeling of the bacterial porin OmpF. *Biophys J* 97:1898–1906.
39. Arbing MA, et al. (2000) Charged residues in surface-located loops influence voltage gating of porin from Haemophilus influenzae type b. *J Membr Biol* 178:185–193.
40. Arbing MA, Hanrahan JW, Coulton JW (2001) Mutagenesis identifies amino acid residues in extracellular loops and within the barrel lumen that determine voltage gating of porin from Haemophilus influenzae type b. *Biochemistry* 40:14621–14628.
41. Scheuring S, et al. (2002) Charting and unzipping the surface layer of Corynebacterium glutamicum with the atomic force microscope. *Mol Microbiol* 44: 675–684.
42. Delcour AH (2003) Solute uptake through general porins. *Front Biosci* 8:d1055–d1071.
43. Todt JC, McGroarty EJ (1992) Acid pH decreases OmpF and OmpC channel size in vivo. *Biochem Biophys Res Commun* 189:1498–1502.
44. Müller A, et al. (1999) Neisserial porin (PorB) causes rapid calcium influx in target cells and induces apoptosis by the activation of cysteine proteases. *EMBO J* 18:339–352.
45. Rowlett VW, et al. (2017) Impact of membrane phospholipid alterations in Escherichia coli on cellular function and bacterial stress adaptation. *J Bacteriol* 199:e00849-16.
46. Glenwright AJ, et al. (2017) Structural basis for nutrient acquisition by dominant members of the human gut microbiota. *Nature* 541:407–411.
47. Delcour AH (2009) Outer membrane permeability and antibiotic resistance. *Biochim Biophys Acta* 1794:808–816.